

## Diffraction of Atoms from a Measurement Induced Grating

Stefan Kunze, Kai Dieckmann, and Gerhard Rempe

*Fakultät für Physik, Universität Konstanz,  
Postfach 5560, D-78434 Konstanz, Germany*  
(Received 15 October 1996)

We report on an experiment with polarized atoms passing a standing light wave, where the atom's position is encoded (entangled) with the excitation amplitude of two long lived electronic states. Position information can be obtained *a posteriori* by measuring the electronic state. If this measurement is performed, the atom is localized in an array of virtual slits. This gives rise to diffraction of the atomic de Broglie waves from a measurement induced amplitude grating, thus showing the back action onto the momentum due to the localization. We further demonstrate experimentally that the encoding can be totally erased. [S0031-9007(97)02677-X]

PACS numbers: 03.75.Be, 03.65.-w, 32.80.Pj, 42.50.-p

Complementarity and the measurement of noncommuting observables represent some of the most nonintuitive ingredients of quantum theory and have been the subject of controversial discussions since the early days. For example, the famous Heisenberg microscope [1,2], as the archetype of a position measurement apparatus, shows how the particle's momentum changes during the interaction with the quantized light field. In this case, the back action onto the particle's momentum occurs at the instant of an irreversible scattering process, even when position information is not obtained from the scattered photon. In contrast to this, a more distinct demonstration of the principle of complementarity can be obtained from recently proposed experiments with virtual slits [3–5], which employ a two-step measurement scheme. In the first step, an entanglement between the position of the particle and the state of a second quantum system is generated by means of a reversible interaction. A subsequent measurement performed on this *second* system allows one to determine the particle's position, while the resulting change of the particle's momentum can be observed without directly affecting the particle.

Several schemes were proposed to produce this entanglement. They all employ a position dependent coupling strength between an atom and a light field [6]. For example, the atom-field interaction in the nodes and antinodes of a near-resonant standing-wave light field in a high-finesse cavity leads to a position dependent phase shift of the light field. The atom's position can be determined by observing the light field after the atom has passed the cavity [3–5], or in real time during the atom-field interaction [7–9]. A similar entanglement can be used to obtain which-path information in a Ramsey-type interferometer [10], or to determine the photon number in a cavity [11]. In this case, atoms in a superposition of two long lived internal states are employed, and the entanglement between the occupation probability of these states and the strength of the radiation field is exploited. We now report on an atom optics experiment where we use a

combination of the described schemes to produce an entanglement between the position of an atom and its internal state.

The main ingredients of our experiment are illustrated in Fig. 1. A delocalized rubidium atom with two long lived hyperfine-structure ground states,  $|a\rangle$  and  $|b\rangle$ , and an optically excited state,  $|c\rangle$ , passes the encoding zone where the entanglement is generated: It consists of a near-resonant optical standing wave, sandwiched between two microwave-(RF) zones. Before the interaction with the fields, the atom is prepared in the state

$$|\psi_i\rangle = \frac{1}{\sqrt{L}} \int_{-L/2}^{L/2} |z\rangle \otimes |a\rangle dz, \quad (1)$$

where  $|z\rangle$  denotes the position eigenfunctions along the  $z$  axis and  $L$  characterizes the size of the wave packet, larger than the optical wavelength  $\lambda = 2\pi/k$ . In the first RF zone, the atom is excited into a coherent superposition of the states  $|a\rangle$  and  $|b\rangle$  by means of a  $\pi/2$  pulse. This gives rise to an atomic dipole moment oscillating at frequency  $\omega_{\text{RF}} = (E_a - E_b)/\hbar$ , where  $E_a$  and  $E_b$  are the energies of the two ground states, respectively. Next, the atom passes the standing-wave light field which couples states  $|a\rangle$  and  $|b\rangle$  to the excited state  $|c\rangle$ . The ac-Stark effect shifts the energies of the two ground states by an amount  $\Delta E_a$  and  $\Delta E_b$ , respectively, where  $\Delta E_{a,b}(z) \propto \cos^2(kz)$ .

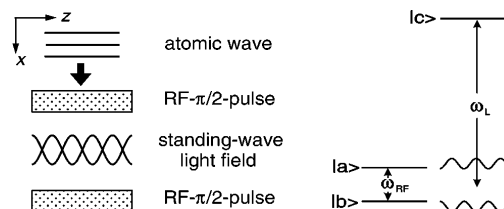


FIG. 1. Principle of the experiment. Left: a delocalized atom passes a standing-wave light field sandwiched by a microwave-(RF)-Ramsey interferometer. Right: simplified level scheme of the atom.

This changes the phase of the atomic dipole moment by

$$\varphi(z) = \frac{1}{\hbar} \int_0^\tau [\Delta E_a(z, t) - \Delta E_b(z, t)] dt = 2\alpha \cos^2(kz),$$

where  $\tau$  is the interaction time. The parameter  $\alpha$  describes the ac-Stark shift at an antinode. It can be adjusted by controlling the intensity and the detuning of the light field. Note that the transverse motion along the  $z$  axis induced by the presence of the light field is neglected during the interaction, i.e., the Raman-Nath approximation is made [12]. Finally, the phase shift  $\varphi(z)$  is transformed into a position dependent occupation probability of states  $|a\rangle$  and  $|b\rangle$  by applying a second RF- $\pi/2$  pulse. When the light frequency  $\omega_L$  is adjusted in order to induce an energy shift  $\Delta E_a(z) = -\Delta E_b(z)$  (see Fig. 1), the outgoing state is [13]

$$|\psi_f\rangle = \frac{1}{\sqrt{2}} \{|\psi^a\rangle + |\psi^b\rangle\}, \quad (2)$$

where

$$|\psi^a\rangle = \frac{\sqrt{2}}{\sqrt{L}} \int_{-L/2}^{L/2} \sin[\varphi(z)/2] |z\rangle \otimes |a\rangle dz,$$

$$|\psi^b\rangle = \frac{\sqrt{2}}{\sqrt{L}} \int_{-L/2}^{L/2} -\cos[\varphi(z)/2] |z\rangle \otimes |b\rangle dz.$$

Equation (2) describes the entanglement between the atom's position  $z$  and its internal state. The state vector of the outgoing atom is a coherent superposition of the two states  $|\psi^a\rangle$  and  $|\psi^b\rangle$  which have different internal states,  $|a\rangle$  and  $|b\rangle$ , and complementary spatial distributions,  $|\psi^a(z)|^2 = \sin^2[\alpha \cos^2(kz)]$  and  $|\psi^b(z)|^2 = \cos^2[\alpha \cos^2(kz)]$ , respectively. A measurement of the internal state of the atom, i.e., a projection onto one of the two states  $|\psi^a\rangle$  or  $|\psi^b\rangle$ , localizes the atom in one or the other of the two spatial distributions. Figure 2 shows the two spatial distributions for  $\alpha = \pi$ . When measuring the atom in the internal state  $|a\rangle$ , for example, the atom is periodically localized as indicated by the solid line, i.e., the atom has passed the displayed amplitude grating. The resulting back action onto the atom's momentum can be regarded as a diffraction from this grating. We emphasize that the grating is not induced before measuring the atom's internal state long after the atom has passed

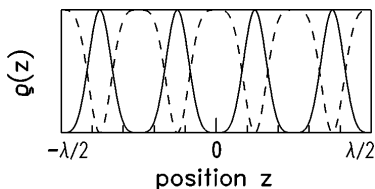


FIG. 2. Localization patterns  $\rho(z)$  of atoms after encoding with  $\alpha = \pi$ . The standing wave has an antinode at  $z = 0$ . The solid curve shows the spatial distribution of atoms detected in state  $|a\rangle$ , corresponding to a localization between the nodes and antinodes of the standing wave. The dashed curve shows the complementary distribution for atoms detected in state  $|b\rangle$ .

the standing-wave light field. A detection of the atom *without* internal state measurement does not give position information. In this case, the momentum distribution reflects only the disturbance of the atomic de Broglie wave due to the interaction with the light field. In contrast to the virtual amplitude grating induced by the localization, this interaction leads to the diffraction of a plane de Broglie wave from a thin phase grating. This results in the well-known Raman-Nath diffraction pattern [14].

The experiment is performed with rubidium atoms of isotope 85. The two states  $F = 3, m_F = 0$  (state  $|a\rangle$ ) and  $F = 2, m_F = 0$  (state  $|b\rangle$ ) of the atomic ground state  $5s^2S_{1/2}$  are used to store the position information. They are coupled to the optically excited  $5p^2P_{3/2}$  state (state  $|c\rangle$ ) by the light of wavelength  $\lambda = 780$  nm. The experimental setup is similar to that described in Ref. [15]. A magneto-optical vapor-cell trap serves as the source of cold rubidium atoms. After trapping, the cloud of atoms is cooled in optical molasses to a temperature below  $10 \mu\text{K}$ . The atoms are then released by switching off all laser light, and move through the vertically aligned setup in free fall. Next, a small magnetic bias field is applied along the horizontal  $y$  direction, which defines the quantization axis. The atoms are then optically pumped into state  $|a\rangle$  with  $\pi$ -polarized laser light, which drives the transition  $5s^2S_{1/2}F = 3 \rightarrow 5p^2P_{3/2}F' = 3$  with  $\Delta m_F = 0$ , and an additional repumping laser on the transition  $5s^2S_{1/2}F = 2 \rightarrow 5p^2P_{3/2}F' = 3$ . (For this configuration, state  $|a\rangle$  is dark due to a vanishing Clebsch-Gordan coefficient.) This allows one to transfer more than 70% of all atoms into state  $|a\rangle$ , while the remaining atoms are distributed over the manifold of states  $5s^2S_{1/2}F = 3$  with  $m_F \neq 0$ .

After optically pumping, the atoms pass the encoding region, which generates the entanglement between the position and the internal state. It is located 20 cm below the trap, where the atoms have a velocity of 2 m/s. To apply the RF field, a rectangular microwave cavity tuned to the atomic transition frequency of  $\omega_{\text{RF}} = 2\pi \times 3.035$  GHz is used. The magnetic field of the  $\text{TE}_{102}$  mode, polarized along the quantization axis, drives the magnetic dipole transition between states  $|a\rangle$  and  $|b\rangle$  and induces a  $\pi/2$  pulse within  $1.1 \mu\text{s}$ . This time is short compared to the transit time of the atoms through the resonator,  $t = 15$  ms, thus allowing one to realize the Ramsey interferometer by applying the two RF pulses while the atoms are located inside the cavity. Between the pulses, the atoms interact with the standing-wave light field, generated by retroreflecting a Gaussian laser beam from a flat mirror, which is mounted inside the microwave resonator. With a laser beam waist of  $\omega_x = 8.2$  mm along the vertical  $x$  direction, the curvature of the wave fronts can be neglected over the size of the atomic cloud. Short interaction times less than  $7 \mu\text{s}$  are required to fulfill the Raman-Nath condition [12]. This is realized by pulsing the light field on when the cloud of falling atoms is located in front of the mirror. The light field is  $\pi$  polarized

and couples state  $|a\rangle$  to the sublevels  $F' = 4, m'_F = 0$  and  $F' = 2, m'_F = 0$ , and state  $|b\rangle$  to the sublevels  $F' = 3, m'_F = 0$  and  $F' = 1, m'_F = 0$  of state  $|c\rangle$ , respectively. The resulting ac-Stark shift of both ground states,  $|a\rangle$  and  $|b\rangle$ , is the sum of the two light shifts due to the two couplings, and the two energy shifts  $\Delta E_{a,b}$  are equal in magnitude but opposite in sign when the light is blue detuned by 1.44 GHz with respect to the frequency of the  $F = 3 \rightarrow F' = 4$  transition. A peak running-wave light intensity of 40 mW/cm<sup>2</sup> induces an energy shift at an antinode of  $\Delta E_a/\hbar = 1.28 \times 10^6$  rad/s. Therefore,  $\alpha = \pi$  is realized by employing a 2.5  $\mu$ s long light pulse.

Finally, the atoms are detected 25 cm below the encoding region by means of spatially resolved fluorescence detection. By choosing the appropriate laser frequencies for the excitation, either atoms in state  $|a\rangle$  or both  $|a\rangle$  and  $|b\rangle$  can be observed. This allows one to record a state-selective momentum distribution of the atomic sample as a Fraunhofer diffraction pattern with a resolution of  $\Delta p = 0.35\hbar k$  (FWHM) [15].

Delocalized atoms with a well-defined vertical velocity  $v_x$  and good spatial coherence are required for the experiment. While sufficient longitudinal coherence of  $v_x/\Delta v_x \approx 40$  (FWHM) is guaranteed by the low temperature of the atomic cloud, high transverse coherence is achieved by collimating the atomic sample using a 200  $\mu$ m wide slit just above the interaction region. The resulting initial momentum width of  $1.5\hbar k$  (FWHM) is due mainly to the finite size of the atomic cloud after molasses cooling [0.7 mm (FWHM)] and some heating during the optical pumping process.

Figure 3 shows the experimental results for  $\alpha = \pi$ . The upper plot displays the momentum distribution obtained without state-selective detection, i.e., all atoms are

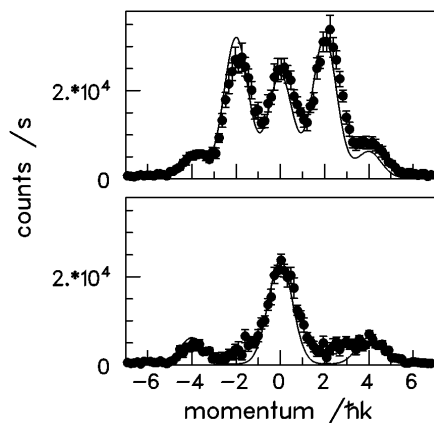


FIG. 3. Measured momentum distribution after encoding with  $\alpha = \pi$ . Upper plot: non-state-selective detection of atoms in state  $|a\rangle$  and  $|b\rangle$  (no localization). The momentum spectrum is due to diffraction from a thin phase grating. Lower plot: state-selective detection of atoms in state  $|a\rangle$ , i.e., projection on state  $|\psi^a\rangle$ . The difference between the upper and lower distribution is due to the localization between the nodes and antinodes of the standing light wave.

detected independent of their internal state. As discussed above, position information cannot be obtained in this case, and the atomic momentum spectrum is due to diffraction from the standing-wave light field with period  $\lambda/2$ . This gives rise to diffraction orders separated by  $2\hbar k$ . The solid line shows the theoretical prediction, taking into account the initial momentum distribution. No adjustable parameter is used to fit the data. The lower plot shows the momentum spectrum recorded with the same control parameters for the position encoding, however, only atoms in state  $|a\rangle$  are detected. Thus the atomic state is projected on state  $|\psi^a\rangle$ , and the atoms are localized halfway between the nodes and antinodes of the standing wave, as indicated in Fig. 2 (solid line). The measurement process effectively produces an amplitude grating with periodicity  $\lambda/4$ , thereby inducing a diffraction pattern with diffraction orders separated by  $4\hbar k$ . The solid line shows the theoretical prediction for the momentum distribution of state  $|\psi^a\rangle$  [13], which is in good agreement with the experimental data.

In order to demonstrate further possibilities of the encoding process, Fig. 4 displays the results of a similar measurement but now, with  $\alpha = 2\pi$  realized, using twice the light intensity. The calculated amplitude grating for atoms detected in state  $|a\rangle$  is shown in the inset of the lower plot. Again, the spatial periodicity is  $\lambda/4$ , but now the narrow double-peaked structure induces a relative phase shift of  $\pi$  on the atomic de Broglie wave. This gives rise to destructive interference in the forward direction and constructive interference into the odd-numbered interference orders  $\pm 2\hbar k, \pm 6\hbar k, \dots$ . This explains the apparent shift of the diffraction pattern. Again, the solid lines show the theoretical predictions.

The measurements clearly demonstrate the back action of the localization onto the momentum. Nevertheless, the experimental results presented so far could also be

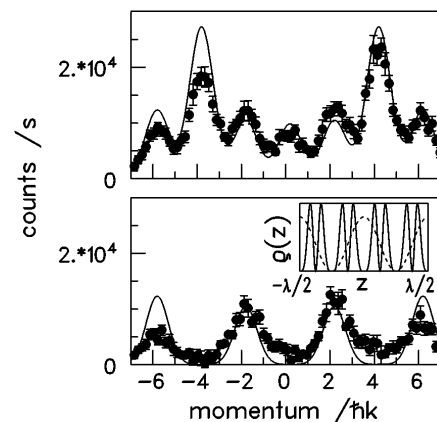


FIG. 4. Measured momentum distribution after encoding with  $\alpha = 2\pi$ . Upper plot: non-state-selective detection. Lower plot: state-selective detection of atoms in state  $|a\rangle$ . The resulting localization pattern is displayed in the inset, where the dashed line indicates the standing wave.

interpreted as a position measurement taking place at the instant of the encoding process. In this case, the atoms would leave the interaction zone not in a coherent superposition of states  $|\psi^a\rangle$  and  $|\psi^b\rangle$  but in one of these states with equal probability. The density matrix would represent the density matrix of a classical mixture of the two states with vanishing off-diagonal elements, and the interaction would not be a reversible *encoding* process but an irreversible *measurement*. To demonstrate the unitary nature of the encoding process, we now show experimentally that it can be totally reversed. A suitable process for this “decoding” is a second sequence, which is identical to the first one used to produce the entanglement and is applied immediately after the first one. Experimentally, this is performed by applying a third RF- $\pi/2$  pulse followed by a second light pulse and a fourth RF- $\pi/2$  pulse, while the atoms are in front of the mirror inside the RF cavity. The total sequence thus consists of a RF- $\pi/2$  pulse and a light pulse, followed by a RF- $\pi$  pulse, another light pulse, and a final RF- $\pi/2$  pulse. The intermediate RF- $\pi$  pulse changes the phase of the atomic dipole moment [ $\varphi(z) \rightarrow -\varphi(z)$ ], so that the phase shift induced by the second interaction with the light field, together with the final RF- $\pi/2$  pulse, restores the atom’s initial state vector. A phase stable RF source has to be used, and the total pulse sequence must be short ( $<10 \mu\text{s}$ ) in order to neglect the motion of the atom.

Figure 5 (stars) shows the momentum distribution of atoms subject to an encoding process with  $\alpha = \pi$  and the subsequent reversal by the decoding sequence. Only atoms in state  $|a\rangle$  are detected. Figure 5 (open circles) shows the result of the non-state-selective detection after *one* encoding process with  $\alpha = \pi$ . (This measurement is identical to the one shown in Fig. 3, upper plot.) By comparing the areas underneath the signals of the two measurements, it is obvious that after the second sequence nearly all atoms are found in state  $|a\rangle$ . In addition, most of the atoms have about zero momentum, i.e., the final momentum distribution resembles the initial one. Thus, the effect of the encoding sequence is totally erased, and the state vector  $|\psi_f\rangle$  is transformed back into the initial state  $|\psi_i\rangle$ , as given by Eq. (1). The small satellites at  $\pm 4\hbar k$  are produced by atoms which are not optically pumped into state  $|a\rangle$ , as was discussed above. These atoms are not affected by the RF-Ramsey pulses because of the Zeeman shift in the magnetic bias field. However, the two consecutive interactions with the light field (each with  $\alpha = \pi$ ) give rise to diffraction from a standing wave with  $\alpha = 2\pi$ , as shown in Fig. 4 (upper curve).

The experiment clearly demonstrates how the entanglement between the atom’s position and its internal state allows one to localize the atom without *directly* affecting the particle’s spatial wave function. In particular, the encoding is a reversible process, while the irreversible back action onto the momentum does not occur before

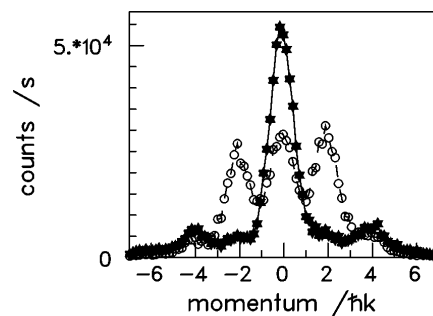


FIG. 5. Measured momentum distribution after encoding with  $\alpha = \pi$  and subsequent erasing with a second, identical process (stars). For comparison, the open circles show the momentum distribution of Fig. 3. The effect of the encoding process is totally erased.

the position information is read out from the atom’s internal states. Besides illustrating the fundamental properties of the quantum-mechanical measurement process, the described localization scheme could have other interesting applications in the field of atom optics. For example, the possibility of producing narrow localization structures with widths below  $\lambda/20$ , together with the high spatial periodicity of the virtual slits, has potential applications in high-resolution atom imaging, atom lithography, and atom interferometry.

We thank S. Dürr for help in the experiment. This work is supported by the Deutsche Forschungsgemeinschaft.

- 
- [1] W. Heisenberg, Z. Phys. **43**, 172 (1927).
  - [2] M. S. Chapman *et al.*, Phys. Rev. Lett. **75**, 3783 (1995).
  - [3] P. Storey, M. Collett, and D. F. Walls, Phys. Rev. Lett. **68**, 472 (1992).
  - [4] M. A. M. Marte and P. Zoller, Appl. Phys. B **54**, 477 (1992).
  - [5] A. M. Herkommer, H. J. Carmichael, and W. P. Schleich, Quantum Semiclass. Opt. **8**, 181 (1996).
  - [6] For a recent review about position measurements, see J. E. Thomas and L. J. Wang, Phys. Rep. **262**, 311 (1995).
  - [7] G. Rempe, Appl. Phys. B **60**, 233 (1995).
  - [8] R. Quadt, M. Collett, and D. F. Walls, Phys. Rev. Lett. **74**, 351 (1995).
  - [9] H. Mabuchi, Q. A. Turchette, M. S. Chapman, and H. J. Kimble, Opt. Lett. **21**, 1393 (1996).
  - [10] M. Brune *et al.*, Phys. Rev. Lett. **77**, 4887 (1996).
  - [11] M. Brune *et al.*, Phys. Rev. Lett. **65**, 976 (1990).
  - [12] For a detailed review about atom optics, see C. S. Adams, M. Sigel, and J. Mlynek, Phys. Rep. **240**, 145 (1994), and references therein.
  - [13] S. Kunze, G. Rempe, and M. Wilkens, Europhys. Lett. **27**, 115 (1994).
  - [14] P. E. Moskowitz, P. L. Gould, S. R. Atlas, and D. E. Pritchard, Phys. Rev. Lett. **51**, 370 (1983).
  - [15] S. Kunze, S. Dürr, and G. Rempe, Europhys. Lett. **34**, 343 (1996).